

RESEARCH ARTICLE | FEBRUARY 19 2025

Hollow cathode electron properties are consistent with marginally stable turbulence

P. J. Roberts   ; Z. A. Brown  ; B. A. Jorns 

 Check for updates

Appl. Phys. Lett. 126, 074103 (2025)

<https://doi.org/10.1063/5.0241476>



Articles You May Be Interested In

Transforming underground to surface mining operation – A geotechnical perspective from case study

AIP Conference Proceedings (November 2021)

Monthly prediction of rainfall in nickel mine area with artificial neural network

AIP Conference Proceedings (November 2021)

Estimation of Karts groundwater based on geophysical methods in the Monggol Village, Saptosari District, Gunungkidul Regency

AIP Conference Proceedings (November 2021)

Hollow cathode electron properties are consistent with marginally stable turbulence

Cite as: Appl. Phys. Lett. **126**, 074103 (2025); doi: [10.1063/5.0241476](https://doi.org/10.1063/5.0241476)

Submitted: 30 September 2024 · Accepted: 7 February 2025 ·

Published Online: 19 February 2025



View Online



Export Citation



CrossMark

P. J. Roberts,^{a)} Z. A. Brown, and B. A. Jorns

AFFILIATIONS

University of Michigan, Ann Arbor, Michigan 48105, USA

^{a)} Author to whom correspondence should be addressed: pjrob@umich.edu

ABSTRACT

The scaling of the electron Mach number in a 20 A class hollow cathode plume is characterized experimentally as a function of the local plasma properties. These local properties are inferred from measurements with an incoherent Thomson scattering diagnostic, configured to measure the axial projection of the electron velocity distribution on the cathode centerline. The time-averaged electron temperatures are found to be 1–2 eV for xenon flow rates between 1.35 and 2.25 mg/s and increase above 5 eV at a lower flow rate of 0.45 mg/s. This transition in temperature corresponds to the cathode's transition from the so-called spot mode to the plume mode. The electron Mach number is found to be between 0.2 and 0.8 for all flow rates. The scaling of the Mach number with the ratio of electron temperature to ion temperature is examined, which reveals a non-monotonic relationship that can be approximately described by the assumption of marginally stable wave growth. The possibility of leveraging this assumption as a zero-equation closure for the electron fluid equations is discussed in the context of past experiments.

Published under an exclusive license by AIP Publishing. <https://doi.org/10.1063/5.0241476>

The onset of plasma instabilities in current-carrying plasmas is a critical driver of momentum and energy transport.^{1–3} This is particularly prevalent in low-temperature devices such as the hollow cathodes employed for space propulsion and materials processing applications.^{4–6} In these systems, an applied potential accelerates electrons away from the cathode, giving rise to an expanding plasma plume. Within this plume, the local electric field sustains a high electron drift relative to the less-mobile ions.^{7,8}

This strong electron drift can serve as an energy source for the growth of plasma instabilities, most notably ion acoustic turbulence.^{9–13} These modes dominate the balance of particle momentum and energy, affecting the cathode's coupling efficiency^{14–16} and ion sputtering rates.^{17–19} In order to predict the performance and lifetime of these devices, the ability to model these kinetic plasma phenomena is, thus, essential. However, direct kinetic simulations are too expensive to be practical, while hydrodynamic engineering models cannot capture these waves from first principles.^{15,20} In order to model hollow cathodes within a fluid framework, it is, therefore, necessary to predict this turbulence's growth and saturation state as a function of the equilibrium electron and ion properties, such as drift energy and temperature.

Quantifying the impact of these instabilities has historically posed a challenge for hollow cathodes. It is common to represent the wave-

induced forces on the electrons as a drag term in a fluid electron momentum balance. This force is proportional to an “anomalous” collision frequency parameter.²¹ However, introducing this fluid coefficient to account for kinetic effects invites a problem of hydrodynamic closure: how should the collision frequency depend on the background plasma properties? To this end, several so-called “closure models” have been proposed to date and experimentally assessed.^{16,22–24} These models depend on assumptions as to the saturated state of the wave amplitudes based on the available growth and damping mechanisms. Despite the effectiveness of this type of closure for other plasma configurations, however, there has yet to be a fully validated model for hollow cathode plumes.

One approach at closure that has not been assessed experimentally for cathodes is the hypothesis of “marginal stability.” Originally advanced by Manheimer,²⁵ this theory assumes that the waves' linear growth and damping mechanisms balance. In this state, amplitudes never reach the more strongly nonlinear Sagdeev saturation limit.²² The marginally stable configuration instead implies an algebraic relationship between the electron drift and temperature, closing the fluid equations.

Evaluating the hypothesis of marginal stability for ion acoustic waves requires measurements of electron fluid properties, such as the Mach number and temperature. In cathodes, directly assessing these

parameters with conventional probes has been challenging.^{13,23,26} Electrical probes yield only radially averaged estimates for the Mach number, and the temperature is sensitive to the probe analysis method.

Incoherent Thomson scattering (ITS) can provide these measurements by directly resolving the electron velocity distribution function (EVDF). Historically, this tool lacked sufficient signal strength to work for low-temperature, low-density plasmas such as cathode plumes. However, Vincent and Tsikata recently demonstrated a system with enough signal to directly resolve the EVDF in a cathode.^{27,28} A similar system was demonstrated on the cathode plume of an operating Hall thruster in Ref. 29. With that said, in these previous measurements, the scattering configuration was not oriented along the device axis and, thus, could not capture the wave-inducing electron drift.³⁰ The Mach number, thus, has yet to be directly characterized with ITS.

The goal of this work is to apply an ITS experiment to capture the cathode's axial electron properties, and from these to assess the hypothesis of marginally stable ion acoustic turbulence. To this end, we first overview the predicted relationship between plasma properties based on the assumption of marginal stability. We then present the experimental setup and results to evaluate this relationship. Finally, we compare the predictions of this wave assumption against experimental data and discuss the implications for closure modeling.

Ion acoustic modes in a current-carrying plasma grow by sapping energy from the strong electron drift. Following Ref. 16, the growth of ion acoustic turbulence in the cathode plume can be described by the imaginary component of the frequency,

$$\omega_i = \sqrt{\frac{\pi k_B T_e}{8 m_i}} k \left[M_e - \left(\frac{T_e}{T_i} \right)^{3/2} \exp \left\{ -\frac{T_e}{2 T_i} \right\} \right] - \frac{\nu_i}{2}, \quad (1)$$

where ω_i is derived from the dispersion relation $\vec{k}(\omega_r + i\omega_i)$. The right-hand side describes effects that cause the waves to either grow or damp. The three terms represent wave growth due to inverse electron Landau damping, ion Landau damping, and damping due to classical electron-ion collisions at frequency ν_i . We ignore these classical collisions from this point forward due to the large collisional mean free path.³¹ In this work, we neglect higher-order nonlinear effects by assuming that the waves saturate before reaching large amplitudes. If the waves are marginally stable within this linear growth model, both sides of Eq. (1) must equal zero. Therefore, the right-hand side of the equation leads to a constraint on the plasma properties,

$$M_e = \left(\frac{T_e}{T_i} \right)^{3/2} \exp \left\{ -\frac{T_e}{2 T_i} \right\}, \quad (2)$$

which effectively “closes” the fluid equations.

To assess the validity of this relationship, we implemented the Incoherent Thomson Scattering (ITS) system shown in Fig. 1(a) to measure the plasma properties in the plume of a 60-A class LaB6 hollow cathode. The cathode carried 20 A of current to a cylindrical anode in a 0.7-m-diameter by 1.5-m vacuum chamber, whereas we varied the xenon flow rate parametrically.^{13,32} Background pressure in the facility remained below 50 μ Torr for all test points.

The ITS system, described further in Ref. 33, consisted of a Q-switched, frequency-doubled Nd:YAG laser, which we focused into the plasma through Brewster window vacuum feedthroughs. A collection lens imaged the scattered light from the 1-mm³ laser focus, which was fiber-coupled to the detection table. We translated the cathode

relative to the intersection point of the collection optic and laser beam with a linear motion stage. On the detection table, two volume Bragg grating filters removed stray laser light at 532 nm, after which the light entered an HRS-750 spectrometer.²⁷ A 1200 grooves/mm grating then dispersed the beam to form an image of the spectrum on a vertically binned EMICCD detector chip with 15 km/s velocity resolution per pixel. The 20-ns detector exposure was synchronized to the 10-Hz laser pulse and operated at a gain of 5000. To improve signal relative to the CCD noise, we applied a photon-counting algorithm based on a detection threshold of 200 counts.^{34,35}

The resulting laser scattering spectrum is a distribution of photon counts over wavelength, λ , around the laser wavelength of $\lambda_0 = 532$ nm. Figure 1(b) shows a typical spectrum, where the Doppler relation, $\nu(\lambda) = c(\lambda_0/\lambda - 1)/(2 \sin(\theta/2))$, converts the scattered wavelength to the velocity.³⁶ Here, c represents the speed of light, and θ represents the angle between the incident and scattered wavevectors, as shown by the inset in Fig. 1(a). The resulting velocity distribution is projected along the axial measurement vector $\Delta \vec{k} = \vec{k}_s - \vec{k}_i$, where k_i denotes the incident wavevector and k_s denotes the scattered wavevector. Dashed lines in Fig. 1(b) denote the velocity band attenuated by the Bragg filters, which is not considered for fitting.

In order to extract electron properties from the EVDF, we assumed a Maxwellian distribution and accounted for convolutional broadening by the spectrometer's instrument function,^{28,33} which we approximated as the laser's unfiltered line shape. Solving the inverse problem for the best-fit parameters n_e , ν_T , and u_d , given this Maxwellian model by way of least squares optimization determines these fluid parameters directly. The calibration factor H determines the absolute intensity, due to laser power and transmission efficiencies.²⁷ We determined H using the rotational Raman scattering spectrum of nitrogen and oxygen molecules in ambient air at a pressure of 0.1 Torr as measured with the same apparatus.^{28,29,33,37}

We show in Fig. 2 the axial electron properties along the cathode axis, referenced to the keeper surface. The error bars show 95% credible intervals based on fitting uncertainty. From these results, we first note that in all cases, the electron density [Fig. 2(a)] decays with distance from the cathode exit. This type of decay has been noted before from measurements performed with physical probing techniques.^{13,38} The decrease with distance is physically consistent with the decrease in density due to the expansion of the plume into vacuum. We also note that the electron density globally appears to increase with the flow rate. Similar features have also been noted in previous studies²⁸ and can be attributed to the fact that higher neutral flow correlates with higher rates of plasma production in the discharge.

In Fig. 2(b), we show the electron temperature. For the two higher flow rate conditions (1.35 and 2.25 mg/s), the value of T_e remains near 1–2 eV. These temperatures are within a factor of two of previously reported data on similarly configured cathodes,¹³ which ranged from 2 to 3.5 at these operating conditions. At the 1.35 mg/s flow rate, the furthest downstream measurement exhibits a marked increase in temperature with a larger error bar. This in large part can be attributed to poor fitting to the lowest-signal measurement in the dataset. In a departure from the high-flow rate conditions, the low-flow case shows temperatures rising from 5 eV near the cathode exit to 8–10 eV at 1 cm downstream of the cathode exit. These temperatures also roughly agree with Langmuir probe measurements and undirected Thomson scattering measurements in the near field, which showed a rise from 2 eV at

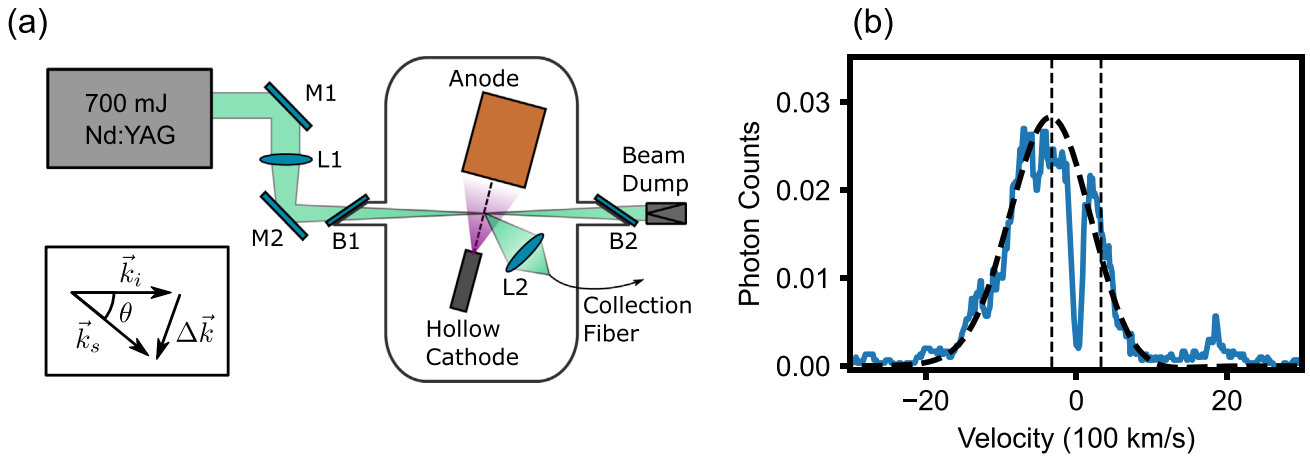


FIG. 1. (a) Schematic of the incoherent Thomson scattering apparatus for obtaining the axial electron velocities. The inset displays the scattering geometry. (b) Example of a typical electron velocity distribution function in the hollow cathode plume, with a Maxwellian fit. The vertical axis unit is average photon counts per laser pulse, where the average is taken over 3000 laser pulses. Vertical lines show the band attenuated by the optical notch filters, which are rejected from fitting.

the cathode exit to 7 eV in the far plume.^{13,29} This increase in temperature was also correlated with a marked increase in low-frequency (~ 10 kHz) oscillations in the cathode current, as measured by an inductive current probe on the discharge power supply. These large oscillations indicate the transition to plume mode, an operating state in cathodes correlated with high currents and low-flow rates with large global oscillations.^{5,39} This mode has been shown in past studies to coexist with increased electron temperatures.

Finally, Fig. 2(c) shows the axial velocities, which are inferred from the shift of the scattered spectrum's mean relative to the laser wavelength. For the high-flow rate conditions, the velocity is relatively constant through the plume, save for some outlier values downstream. These values could be an artifact of the decreased signal-to-noise in the far field, as reflected by the larger error bars. For example, while at 5 mm, the signal-to-noise ratio (SNR) exceeds 25 for a flow rate of 1.35 mg/s, at 20 mm, the SNR falls to around 0.5, and noise can artificially broaden the distribution.²⁹ At the lowest-flow condition, the apparent velocity varies non-monotonically throughout the plume. However, the spatially averaged velocity monotonically decreases as

the flow rate is increased. Physically, this trend can be explained by particle continuity: when the plasma density is increased at higher flow rates, the electron drift speed must decrease to support the same current.

Armed with this experimental plasma property data, we can now evaluate the validity of the marginal stability relationship [Eq. (2)] for describing the relationship between these properties. In Fig. 3, we show the scaling of the electron Mach number, $M_e = u_d/v_{Te}$, against the electron temperature to ion temperature ratio for the measurements across all operating conditions. The magnitudes of the reported Mach numbers are broadly consistent with the values that have previously been inferred from indirect probe-based measurements, though the values we report are up to a factor of two lower.^{23,26} Notably, the average magnitude of the electron Mach number is not monotonic with flow rate or electron temperature. The Mach number is below 0.5 for the 0.45 and 2.25 mg/s conditions, while at 1.35 mg/s, the electron drift is a larger fraction of the thermal speed ($M_e \geq 0.5$).

We also show in Fig. 3 an evaluation of Eq. (2), the marginal stability relationship. We lack direct measurements of the ion

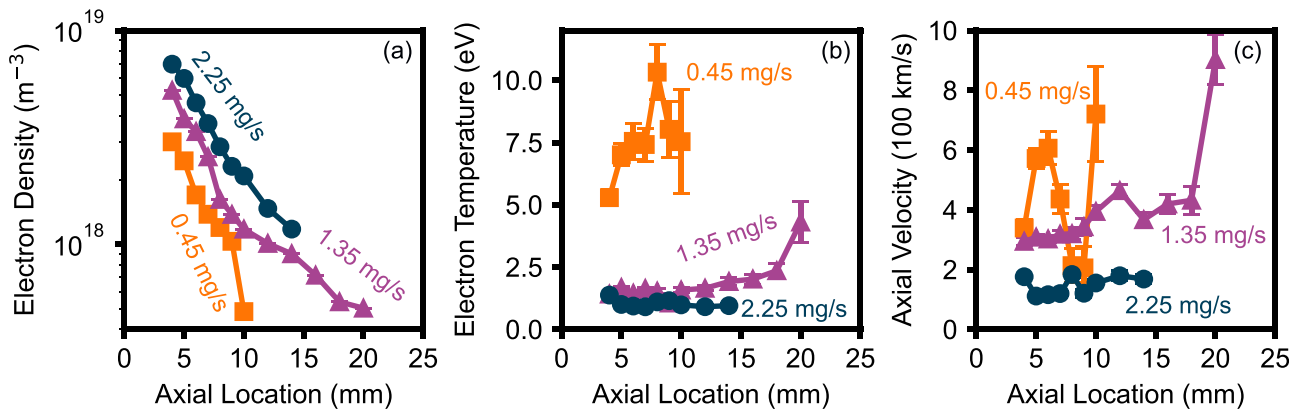


FIG. 2. Fluid properties inferred from the fits to the Thomson scattering spectra along the axial direction. (a) Plasma density. (b) Electron temperature. (c) Electron drift speed.

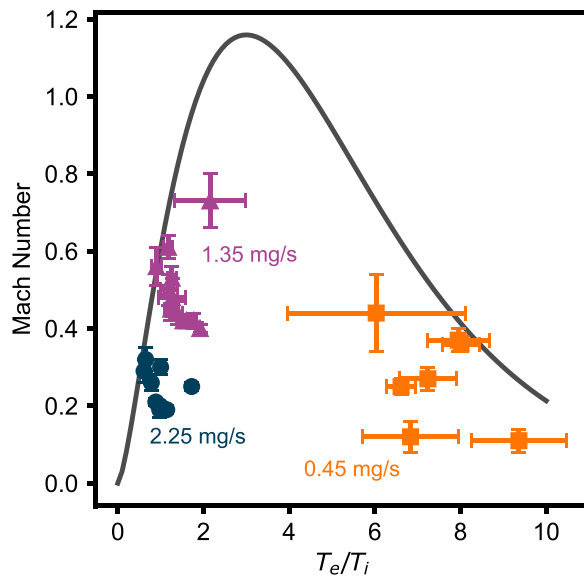


FIG. 3. Mach number vs electron-to-ion temperature ratio for all of the data acquired in the study. Overlaid is the relationship derived assuming marginally stable ion acoustic turbulence. The ion temperature is assumed to increase linearly with position from 0.5 eV at the cathode exit to 2 eV at 20 mm.

temperature, but based on past experiments on similar devices, this quantity likely increases with distance from the cathode.^{18,26,40,41} Based on our near-field ion temperature measurements in a previous study on a similar cathode, we approximate the growing ion temperature as a linear function with distance, having a value of 0.5 eV at the cathode exit and 2 eV at 20 mm.⁴¹ We note, however, that higher-current cathodes in the “plume mode” can demonstrate even more rapid ion heating.¹⁸ Studies with retarding potential analyzers have also shown the presence of higher-energy ions due to wave heating in the downstream region and the bulk drift of the ions.¹⁸ We see that across operating conditions, the marginal stability fit captures well the non-monotonic variation of the Mach number with the electron-to-ion temperature ratio, including the sharp increase in Mach number with temperature ratio at high-flow rates and gradual decrease at low-flow rates.

Given that the assumption of marginal IAT stability captures the scaling of cathode plume plasma properties at multiple operating conditions and across the spot-to-plume-mode transition, we now explore the theoretical implications of this relationship for closure of the electron fluid momentum equation in the context of previous measurements. The force exerted by the wave fields on the electrons can be written as an effective drag force per unit volume, $f_e = -m_e n_e u_{ez} \nu_{AN}$, where ν_{AN} is the anomalous collision frequency. For ion acoustic waves with energy density W_T and a frequency on the order of the ion plasma frequency,^{13,16,26,42} this term takes the following form:

$$\nu_{AN} = \sqrt{\frac{\pi}{16}} \eta \frac{\omega_{pe} W_T}{n_e k_B T_e}, \quad (3)$$

where η is a scaling constant of order 1 and ω_{pe} is the electron plasma frequency.

In order to evaluate this wave force, we still require an assumption for the saturation energy density of the waves. Two common such

assumptions are that the waves saturate at some fraction ε of the local electron thermal energy density, $W_T = \varepsilon n_e k_B T_e$, or the electron drift kinetic energy, $W_T = \varepsilon m_e n_e u_{ez}^2$ for a constant ε of order unity. For the case of thermal saturation, the collision frequency is independent of Mach number and temperature, and, thus, the marginal stability relationship would only affect the energy balance rather than the momentum-transfer collision frequency.

However, in the case of drift-energy-saturated-waves, the temperature-dependence remains; substituting Eq. (2) for marginally saturated turbulence yields

$$\nu_{AN,Drift} = \zeta \omega_{pe} \left(\frac{T_e}{T_i} \right)^3 \exp \left\{ \frac{-T_e}{T_i} \right\}, \quad (4)$$

where ζ is a constant. This formulation implicitly includes the assumption that the wave growth is described by weak, collisionless turbulence theory. As a result, the functional form of the effective collision rate scales strongly with the rate of linear ion Landau damping, which, in turn, scales with T_e/T_i . Notably, in a previous experimental study of the time-resolved plasma properties in this cathode, this saturation assumption led to the only closure model, which could qualitatively predict the fluctuations in electron properties.²⁴

We can also compare these results inferred from plasma properties with previous experimental studies that aimed to measure the wave properties directly in hollow cathodes. Recent probe measurements of wave growth rates on a similar cathode demonstrated only minor deviations from the linear theory,⁴³ which is consistent with our prediction that the waves saturate before reaching nonlinear amplitudes. Similar probe measurements in a $5\times$ higher-current cathode, however, suggested higher Mach numbers and unsaturated wave amplitudes in the near field.²⁶ At the same time, coherent Thomson scattering measurements of the wave spectrum in a lower-power cathode instead revealed evidence of nonlinear interactions shaping the wave spectrum.⁴⁴ Taken together, these studies suggest that a fully predictive model of the wave saturation state should depend on the global discharge parameters and device geometry.

Furthermore, we note that other plasma configurations have similarly been observed to exhibit anomalous transport governed by marginally stable ion turbulence, including the Earth’s ion acoustic bow shock⁴⁵ and suprathermal ion structures in tokamaks.⁴⁶ Despite this agreement of marginal stability theory with the plasma properties, we note that our quantitative results could be altered if the assumptions that ion temperature is below 2 eV and nonlinear wave interactions are small do not hold. Also, we remind the reader that low-frequency plasma fluctuations, especially in the plume-mode operating condition at 0.45 mg/s, could lead to blurring on the time-averaged Thomson spectra, which artificially increases apparent temperatures.⁴⁷ However, these admissions would result in only minor modifications to the strongly non-monotonic dependence of Mach number on temperature. Formulating the wave saturation properties algebraically is a step toward not only predictive modeling of these devices, but potentially mitigation of strong instabilities that affect performance, which has been possible in other plasma configurations.⁴⁸

In summary, we have non-intrusively measured the axial projection of the electron velocity distribution in a hollow cathode plume. We inferred the electron temperature, density, and velocity from this measurement assuming thermodynamic equilibrium. We found that the Mach number, which strongly influences the wave modes which

can grow, was moderate—between 0.3 and 0.8 in all cases. We then invoked the hypothesis that the ion acoustic waves that are known to exist in the cathode plume are marginally stable, leading to a relationship between the Mach number and the ratio of electron temperature to ion temperature. This simple method for describing the wave saturation state explains the observed non-monotonic trends in electron properties well, including across the transition from the spot mode to the plume mode. As a result, this relationship offers a potential closure to the electron fluid equations, allowing self-consistent simulations of the plasma properties. To this end, we demonstrated the resulting functional forms for the anomalous collision rate parameter based on various assumptions for the wave energy saturation level. If these expressions prove to be generalizable across different cathode configurations, this approach offers a potential solution to the problem of predicting hollow cathode anomalous electron resistivity.

This work was supported by a NASA Space Technology Graduate Research Opportunity (Grant No. 80NSSC20K1229), the Air Force through a DURIP (Grant No. FA9550-20-1-0191), and the Joint Advance Propulsion Institute, a NASA Space Technology Research Institute (Grant No. 80NSSC21K1118).

AUTHOR DECLARATIONS

Conflict of Interest

The authors have no conflicts to disclose.

Author Contributions

P. J. Roberts: Conceptualization (equal); Data curation (lead); Formal analysis (lead); Funding acquisition (equal); Methodology (equal); Software (lead); Writing – original draft (lead); Writing – review & editing (lead). **Z. A. Brown:** Conceptualization (equal); Funding acquisition (equal); Methodology (equal); Software (supporting); Writing – review & editing (supporting). **B. A. Jorns:** Conceptualization (equal); Funding acquisition (lead); Methodology (equal); Project administration (lead); Supervision (lead); Writing – review & editing (equal).

DATA AVAILABILITY

The data that support the findings of this study are available from the corresponding author upon reasonable request, subject to US export control restrictions.

REFERENCES

- A. M. Lietz, E. Johnsen, and M. J. Kushner, “Plasma-induced flow instabilities in atmospheric pressure plasma jets,” *Appl. Phys. Lett.* **111**, 114101 (2017).
- S. Hepner, B. Wachs, and B. Jorns, “Wave-driven non-classical electron transport in a low temperature magnetically expanding plasma,” *Appl. Phys. Lett.* **116**, 263502 (2020).
- I. Desjardin, K. Hara, and S. Tsikata, “Self-organized standing waves generated by ac-driven electron cyclotron drift instabilities,” *Appl. Phys. Lett.* **115**, 234103 (2019).
- H. Baránková, L. Bardos, and A. Bardos, “Magnetized hollow cathode activated magnetron,” *Appl. Phys. Lett.* **107**, 153501 (2015).
- D. M. Goebel, I. Katz, and I. G. Mikellides, *Fundamentals of Electric Propulsion* (John Wiley & Sons, 2023).
- S. Muhl and A. Pérez, “The use of hollow cathodes in deposition processes: A critical review,” *Thin Solid Films* **579**, 174–198 (2015).
- P. F. Little and A. Von Engel, “The hollow-cathode effect and the theory of glow discharges,” *Proc. R. Soc. London. Ser. A* **224**, 209–227 (1954).
- C. Ferreira and J. Delcroix, “Theory of the hollow cathode arc,” *J. Appl. Phys.* **49**, 2380–2395 (1978).
- T. E. Stringer, “Electrostatic instabilities in current-carrying and counter-streaming plasmas,” *J. Nucl. Energy, Part C* **6**, 267–279 (1964).
- G. A. Csiky, *Measurements of Some Properties of a Discharge from a Hollow Cathode* (National Aeronautics and Space Administration, 1969), Vol. 4966.
- D. Siegfried and P. Wilbur, “An investigation of mercury hollow cathode phenomena,” in *13th International Electric Propulsion Conference* (ERPS, 1978), p. 705.
- M. Mandell and I. Katz, “Theory of hollow operation in spot and plume modes,” in *30th Joint Propulsion Conference and Exhibit* (AIAA, 1994), p. 3134.
- M. P. Georgin, “Ionization instability of the hollow cathode plume,” Ph.D. thesis (University of Michigan, 2020).
- C. Zhong, H. Li, Y. Hu, Z. Wang, Y. Ding, L. Wei, and D. Yu, “Radial position effects of externally mounted hollow cathode on a magnetically shielded hall thruster,” *Appl. Phys. Lett.* **121**, 264101 (2022).
- I. G. Mikellides, I. Katz, D. M. Goebel, and K. K. Jameson, “Evidence of non-classical plasma transport in hollow cathodes for electric propulsion,” *J. Appl. Phys.* **101**, 063301 (2007).
- A. Lopez Ortega, B. A. Jorns, and I. G. Mikellides, “Hollow cathode simulations with a first-principles model of ion-acoustic anomalous resistivity,” *J. Propul. Power* **34**, 1026–1038 (2018).
- D. M. Goebel, K. K. Jameson, I. Katz, and I. G. Mikellides, “Potential fluctuations and energetic ion production in hollow cathode discharges,” *Phys. Plasmas* **14**, 103508 (2007).
- C. A. Dodson, D. Perez-Grande, B. A. Jorns, D. M. Goebel, and R. E. Wirz, “Ion heating measurements on the centerline of a high-current hollow cathode plume,” *J. Propul. Power* **34**, 1225–1234 (2018).
- I. G. Mikellides, I. Katz, D. M. Goebel, K. K. Jameson, and J. E. Polk, “Wear mechanisms in electron sources for ion propulsion, ii: discharge hollow cathode,” *J. Propul. Power* **24**, 866–879 (2008).
- I. Mikellides, I. Katz, D. Goebel, and J. Polk, “Theoretical modeling of a hollow cathode plasma for the assessment of insert and keeper lifetimes,” AIAA Paper No. 2005-4234, 2005.
- R. Davidson and N. Krall, “Anomalous transport in high-temperature plasmas with applications to solenoidal fusion systems,” *Nucl. Fusion* **17**, 1313–1372 (1977).
- R. Z. Sagdeev and A. A. Galeev, *Nonlinear Plasma Theory* (W. A. Benjamin, Inc., 1969), pp. 37–54.
- M. P. Georgin, B. A. Jorns, and A. D. Gallimore, “Transient non-classical transport in the hollow cathode plume I: Measurements of time-varying electron collision frequency,” *Plasma Sources Sci. Technol.* **29**, 105010 (2020).
- M. P. Georgin and B. A. Jorns, “Transient non-classical transport in the hollow cathode plume ii: Evaluation of models for the anomalous collision frequency,” *Plasma Sources Sci. Technol.* **29**, 105011 (2020).
- W. M. Manheimer and R. Flynn, “Anomalous resistivity and ion-acoustic turbulence,” *Phys. Rev. Lett.* **27**, 1175–1179 (1971).
- B. A. Jorns, C. Dodson, D. M. Goebel, and R. Wirz, “Propagation of ion acoustic wave energy in the plume of a high-current LaB₆ hollow cathode,” *Phys. Rev. E* **96**, 023208 (2017).
- B. Vincent, S. Tsikata, S. Mazouffre, T. Minea, and J. Fils, “A compact new incoherent Thomson scattering diagnostic for low-temperature plasma studies,” *Plasma Sources Sci. Technol.* **27**, 055002 (2018).
- B. Vincent, S. Tsikata, G.-C. Potrivitu, L. Garrigues, G. Sary, and S. Mazouffre, “Electron properties of an emissive cathode: Analysis with incoherent Thomson scattering, fluid simulations and Langmuir probe measurements,” *J. Phys. D* **53**, 415202 (2020).
- J. L. Suazo Betancourt, N. Butler-Craig, J. Lopez-Uricoechea, J. Bak, D. Lee, A. M. Steinberg, and M. L. Walker, “Thomson scattering measurements in the krypton plume of a lanthanum hexaboride hollow cathode in a large vacuum test facility,” *J. Appl. Phys.* **135**, 083302 (2024).
- B. A. Jorns, I. G. Mikellides, and D. M. Goebel, “Ion acoustic turbulence in a 100-A LaB₆ hollow cathode,” *Phys. Rev. E* **90**, 063106 (2014).
- A. Lopez Ortega and I. G. Mikellides, “The importance of the cathode plume and its interactions with the ion beam in numerical simulations of hall thrusters,” *Phys. Plasmas* **23**, 043515 (2016).
- R. R. Hofer, S. E. Cusson, R. B. Lobbia, and A. D. Gallimore, “The H9 magnetically shielded hall thruster,” in *35th International Electric Propulsion Conference* (Electric Rocket Propulsion Soc., 2017), pp. 2017–232.

- ³³P. J. Roberts and B. A. Jorns, "Laser measurement of anomalous electron diffusion in a crossed-field plasma," *Phys. Rev. Lett.* **132**, 135301 (2024).
- ³⁴A. G. Basden, C. A. Haniff, and C. D. Mackay, "Photon counting strategies with low-light-level CCDs," *Mon. Not. R. Astron. Soc.* **345**, 985–991 (2003).
- ³⁵P. J. Roberts and B. Jorns, "Characterization of electron Mach number in a hollow cathode with Thomson scattering," AIAA Paper No. 2023-0843, 2023.
- ³⁶D. Froula, S. H. Glenzer, and N. C. Luhmann, Jr., *Plasma Scattering of Electromagnetic Radiation* (Academic Press, New York, 2010), Vol. 30.
- ³⁷M. J. van de Sande, "Laser scattering on low temperature plasmas: High resolution and stray light rejection," *Ph.D. thesis* (Technische Universiteit Eindhoven, 2002).
- ³⁸D. M. Goebel, K. K. Jameson, R. M. Watkins, I. Katz, and I. G. Mikellides, "Hollow cathode theory and experiment. I. Plasma characterization using fast miniature scanning probes," *J. Appl. Phys.* **98**, 113302 (2005).
- ³⁹D. M. Goebel, K. K. Jameson, I. Katz, and I. G. Mikellides, "Plasma potential behavior and plume mode transitions in hollow cathode discharges," in *International Electric Propulsion Conference (IEPC Paper)*, Vol. 277 (2007).
- ⁴⁰G. J. Williams, T. B. Smith, M. T. Domonkos, A. D. Gallimore, and R. P. Drake, "Laser-induced fluorescence characterization of ions emitted from hollow cathodes," *IEEE Trans. Plasma Sci.* **28**, 1664–1675 (2000).
- ⁴¹P. J. Roberts, B. A. Jorns, and V. H. Chaplin, "Experimental characterization of wave-induced azimuthal ion velocities in a hollow cathode plume," AIAA Paper No. 2022-1561, 2022.
- ⁴²R. Z. Sagdeev, "The 1976 Oppenheimer lectures: Critical problems in plasma astrophysics. I. Turbulence and nonlinear waves," *Rev. Mod. Phys.* **51**, 1–9 (1979).
- ⁴³M. F. Liu and B. A. Jorns, "Liu_iepc_2024.pdf," in *38th International Electric Propulsion Conference* (Electric Rocket Propulsion Society, Toulouse, France, 2024), Paper No. IEPC-2024-366.
- ⁴⁴S. Tsikata, K. Hara, and S. Mazouffre, "Characterization of hollow cathode plasma turbulence using coherent Thomson scattering," *J. Appl. Phys.* **130**, 243304 (2021).
- ⁴⁵E. Greenstadt, V. Formisano, C. Russell, M. Neugebauer, and F. Scarf, "Ion acoustic stability analysis of the Earth's bow shock," *Geophys. Res. Lett.* **5**, 399–402, <https://doi.org/10.1029/GL005i005p00399> (1978).
- ⁴⁶R. Nazikian, G. Fu, M. Austin, H. Berk, R. Budny, N. Gorelenkov, W. Heidbrink, C. Holcomb, G. Kramer, G. McKee *et al.*, "Intense geodesic acoustic modes driven by suprathermal ions in a tokamak plasma," *Phys. Rev. Lett.* **101**, 185001 (2008).
- ⁴⁷V. Chaplin, R. Lobbia, A. Lopez Ortega, I. Mikellides, R. Hofer, J. Polk, and A. Friss, "Time-resolved ion velocity measurements in a high-power Hall thruster using laser-induced fluorescence with transfer function averaging," *Appl. Phys. Lett.* **116**, 234107 (2020).
- ⁴⁸J. Simmonds and Y. Raites, "Mitigation of breathing oscillations and focusing of the plume in a segmented electrode wall-less Hall thruster," *Appl. Phys. Lett.* **119**, 213501 (2021).